Development of Early Tissue Cysts and Associated Pathology of *Besnoitia besnoiti* in a Naturally Infected Bull (*Bos taurus*) from South Africa

Author(s): J. P. Dubey , E. van Wilpe , D. J. C. Blignaut , G. Schares , and J. H. Williams
Source: Journal of Parasitology, 99(3):459-466. 2013.
Published By: American Society of Parasitologists
DOI: http://dx.doi.org/10.1645/12-128.1
URL: http://www.bioone.org/doi/full/10.1645/12-128.1

J. Parasitol., 99(3), 2013, pp. 459–466

DEVELOPMENT OF EARLY TISSUE CYSTS AND ASSOCIATED PATHOLOGY OF *BESNOITIA BESNOITI* IN A NATURALLY INFECTED BULL (*BOS TAURUS*) FROM SOUTH AFRICA

J. P. Dubey, E. van Wilpe*, D. J. C. Blignaut†, G. Schares‡, and J. H. Williams§

United States Department of Agriculture, Agricultural Research Service, Beltsville Agricultural Research Center, Animal Parasitic Diseases Laboratory, Building 1001, BARC-East, Beltsville, Maryland 20705-2350. Correspondence should be sent to: *Jitender.dubey@ars.usda.gov*

ABSTRACT: *Besnoitia besnoiti* is an apicomplexan that causes serious economic loss in cattle in many countries and the disease is now spreading in Europe. At least 2 phases of bovine besnoitiosis are recognized clinically. An acute febrile phase characterized by anasarca and necrosis of skin is associated with multiplication of tachyzoites in vascular endothelium; this phase is short-lived and rarely diagnosed. Chronic besnoitiosis characterized by dermal lesions is associated with the presence of macroscopic tissue cysts and is easily diagnosed. Here we report the development of early *B. besnoiti* tissue cysts in a naturally infected Hugenoot bull from South Africa. Tissue cysts were 10–70 μm in diameter, contained 1–12 bradyzoites, and were most numerous in the dermis, testicles, and pampiniform venous plexus. Amylopectin granules in bradyzoites stained red with periodic acid Schiff (PAS) reaction. Bradyzoites varied in size and in the intensity of PAS reaction (some were PAS-negative), some were plump, and others were slender. With immunohistochemical staining with *Besnoitia oryctofelisi* and bradyzoite-specific antibodies (BAG-1 made against *Toxoplasma gondii* bradyzoites), the staining was confined to parasites, and all intracystic organisms were BAG-1 positive. With Gomori's silver stain only bradyzoites were stained very faintly whereas the rest of the tissue cyst was unstained. Ultrastructurally many tissue cysts contained dead bradyzoites and some appeared empty. Unlike bradyzoites from mature cysts, bradyzoites in the present case contained few or no micronemes. These findings are of diagnostic significance. Ultrastructually host cyst cells had features of myofibroblasts, and immunohistochemistry using antibodies against MAC387, lysozyme, vimentin, Von Willebrand factor, and smooth muscle actin confirmed this. Polymerase chain reaction on DNA extracted from lymph node of the bull confirmed *B. besnoiti* diagnosis. Associated clinical findings, lesions, and histopathology are briefly presented. The bull died of nephrotic syndrome; anasarca in acute besnoitiosis due to protein-losing glomerulopathy is a finding not previously reported in cattle.

Species of the apicomplexan genus *Besnoitia* parasitize cattle, goats, equids, reindeer, caribou, opossums, rabbits, rodents, and lizards (Dubey, Sreekumar et al., 2003; Dubey and Yabsley, 2010). To date, 10 species in the genus have been named: *Besnoitia bennetti*, *Besnoitia jellisoni*, *Besnoitia wallacei*, *Besnoitia tarandi*, *Besnoitia darlingi*, *Besnoitia caprae*, *Besnoitia besnoiti* (type species), *Besnoitia oryctofelisi*, *Besnoitia akodoni*, and *Besnoitia neotomofelis* (reviewed in Dubey, Sreekumar et al., 2003; Dubey and Yabsley, 2010). Considerable uncertainty exists, however, regarding the identity of some of these species because the life cycles of only 4 (*B. darlingi*, *B. wallacei*, *B. oryctofelisi*, and *B. neotomofelis*) of these species are known, and morphological differences among the remaining species are poorly defined (Dubey, Sreekumar et al., 2003).

Among all species of *Besnoitia*, *B. besnoiti* is the most pathogenic to domestic animals; this protist causes economic loss in cattle in many countries, particularly Africa, and the parasite is now spreading in Europe (Besnoit and Robin, 1912; Pols, 1960; Bigalke, 1968; Basson et al., 1970; Bigalke and Prozesky, 2004; Cortes et al., 2006; Fernández-García et al., 2009; Mehlhorn et al., 2009; Schares et al., 2009; European Food Safety Authority, 2010; Jacquit et al., 2010; Majzoub et al., 2010; Rostaher et al., 2010; Gentile et al., 2012). Besnoitiosis is usually recognized as a chronic disease. An acute stage characterized by fever, generalized edema, and necrosis of epidermis is thought to result from vasculitis caused by proliferation of tachyzoites in vascular endothelium (Basson et al., 1970; Bigalke and Prozesky, 2004; Gollnick et al., 2013). Pyrexia may be accompanied by anorexia and photophobia (Bigalke and Prozesky, 2004). The acute stage is, however, rarely diagnosed naturally or verified histologically (Basson et al., 1970). The clinical signs seen most commonly are scleroderma, particularly of hind limbs, and orchitis leading to sterility in bulls. Tissue cyst formation is associated with chronic besnoitiosis (Bigalke and Prozesky, 2004).

Basson et al. (1970) described development of tissue cysts in cattle inoculated intravenously with billions of cultured *B. besnoiti* tachyzoites. Very early cysts, measuring 15–25 μm, were seen 11 days post-inoculation (PI). Tissue cysts measuring 30–100 μm were reported in animals at 16–25 days PI. The development of tissue cysts and associated clinical and pathological findings of *B. besnoiti* in a naturally infected bull are reported, the first such study from a naturally infected host of *Besnoitia*.

MATERIALS AND METHODS

Naturally infected bull

A 4-yr-old Hugenoot stud bull (*Bos taurus*) had a sudden onset of increased respiratory effort and localized swellings over the dorsal area of nose including the lips, brisket, and scrotum. Pulse and rectal temperature were within normal limits. Among the differential diagnoses an allergic reaction, ingestion of poisonous plants, or snake bite were considered. Initial symptomatic treatment with corticosteroids (Dexa 0.2, Virbac RSA, Halfway House 1685, South Africa) and an antibiotic, non-steroidal, anti-inflammatory combination (Resflor®, MSD Animal Health, Isando 1600, South Africa) was given. Following a 24-hr observation period the edema was unchanged. Serum was analyzed for albumin, globulin, total protein, urea, creatinine, serum phosphate, serum calcium, and cholesterol by the referring veterinarian. Moderate hypoalbuminaemia (19 g/L, reference range 28–37 g/L), mild hyperglobulinaemia (47 g/L, reference range 28–42 g/L), elevated urea (14.2 mmol/L, reference range 3.6–10.7 mmol/L) and creatinine (197 μmol/L, reference range 10–133 μmol/L), moderate hypocholestrolaemia (0 mmol/L, reference range 1.3–3.8 mmol/L), mild hypocalcaemia (1.69 mmol/L, reference range 2.0–2.9

Received 5 November 2012; revised 14 January 2013; accepted 17 January 2013.

* Departments of Anatomy and Physiology, Faculty of Veterinary Science, University of Pretoria, Onderstepoort, 0110, South Africa.

† Department of Production Animal Studies, Faculty of Veterinary Science, University of Pretoria, Onderstepoort, 0110, South Africa.

‡ Friedrich-Loeffler-Institut, Südufer 10, D-17493 Greifswald-Insel Riems, Germany.

§ Department of Paraclinical Sciences, Faculty of Veterinary Science, University of Pretoria, Onderstepoort, 0110, South Africa.

DOI: 10.1645/12-128.1

mmol/L), and mild hypophosphataemia (1.03 mmol/L, reference range 1.2–2.3 mmol/L) were recorded. Other parameters were within normal reference ranges. The bull was then treated with penicillin, florfenicol (Nuflor®, MSD Animal Health), flunixin (Finadyne®, MSD Animal Health), and thiotic acid (Tioctan Vet®, Bayer Animal Health, Isando 1600, South Africa). Within 6 days testicular degeneration was suspected, with the scrotal skin and skin over edematous areas and limbs hardened and thickened. The bull was treated with tulathromycin (Draxxin®, Pfizer, Sandton 2146, South Africa). No improvement of the clinical signs was observed and chronic weight loss, despite a continued appetite, warranted referral to the Onderstepoort Veterinary Academic Hospital, Pretoria, South Africa. Upon admission, a skin biopsy from apparently affected skin was taken but lesions and parasites were not seen. Routine hematological and biochemical analyses were performed on blood samples. The bull developed severe progressive hypoalbuminaemia (11.8 g/L, reference range 28–37 g/L) and anasarca prior to its demise. Mild leucocytosis (14.09×10^9/L, reference range 4–10×10^9/L) on hemogram was ascribed to previous cortisone treatment and possible secondary infection from open, cracked skin lesions. Microscopic examination of a second biopsy taken 5 days later (5 days prior to death) revealed epidermal necrosis, as if congealed, without inflammatory reaction and with occasional early *Besnoitia* cysts. The course of the disease until death was approximately 21 days; the bull died on 9 April 2012. Necropsy was performed and tissues preserved for histopathology, immunohistochemistry, and electron microscopy. Fresh unfixed spleen, lymph node, and nasopharyngeal mucosal tissue on ice were tested at the Onderstepoort Veterinary Institute, Department of Molecular Biology, by real-time polymerase chain reaction (RT-PCR) for alcelaphine and ovine gammaherpes viruses causing malignant catarrhal fever.

Necropsy and histopathological examination

Samples of affected skin (from fore and hind limbs, sternum, and scrotum), testis, epididymis, prefemoral, superficial cervical and inguinal lymph nodes, heart with coronary fat, lung, spleen, kidneys, brain, nasopharyngeal mucosa, tongue, sublingual and gluteal muscles, and intestines were fixed in 10% neutral buffered formalin. Paraffin-embedded sections were cut at 5 μm and examined after staining with hematoxylin and eosin (H&E) or periodic acid Schiff (PAS) reaction and counterstained with hematoxylin (PASH) or a silver impregnation (Gomori's) stain.

Transmission electron microscopy (TEM)

Formalin-fixed tissue from pampiniform plexus was processed for TEM using standard techniques. Briefly, the samples were post-fixed in 1% osmium tetroxide in Millonig's buffer (pH 7.4), rinsed in the same buffer, dehydrated through graded ethanol into absolute ethanol, and infiltrated with an epoxy resin–propylene oxide mixture before being embedded in absolute resin and polymerized at 60 C overnight. Ultrathin resin sections were contrasted with uranyl acetate and lead citrate and examined in a Philips CM10 TEM operated at 80 kV (FEI Company, Eindhoven, The Netherlands). Seventy-three tissue cysts were studied by TEM; some may have been deeper parts of the same cyst.

"Popped-off" histology sections (Hayat, 2000) from areas of coronary fat, renal cortical blood vessels, and deep scrotal subcutaneous plus epididymal thrombosed blood vessels were re-embedded for TEM. Retrospectively, wax block material of fully developed cutaneous tissue cysts from a chronic bovine *Besnoitia* case from South Africa was deparaffinized for TEM for comparison of fully developed tissue cysts and the young cysts in the present case.

Immunohistochemical (IMH) staining

Staining for Besnoitia antigens: Two types of antibodies were used for IMH staining of parasites. Polyclonal anti-*B. oryctofelisi* antibody (rabbit No. 1, Dubey, Sreekumar et al., 2003) was diluted 1:5,000. Bradyzoite-specific rabbit antibody (BAG-1, also called BAG-5), directed against a heat-shock protein from *Toxoplasma gondii* (McAllister et al., 1996), was used at a 1:1,000 dilution. These antibodies were from the rabbits described in these citations. Staining was performed as described previously (Dubey and Sreekumar, 2003).

Staining for other pathogens: IMH staining of inguinal lymph node, spleen, scrotal skin, small intestine, testis, lung, heart, and brain with bovine viral diarrhea (BVD) antibody (Cornell University, Ithaca, New York) was done at a dilution of 1:2,000. All IMH staining was done with simultaneous staining of known positive-control sections and for some of the cell markers using internal controls.

Staining for host tissue antigens: Using the avidin–biotin immunoperoxidase technique as previously described (Haines and Chelack, 1991), manual IMH staining of heart, scrotal skin, testis, and nasophayngeal mucosa was done with antibody MAC387 (DAKO, Glostrup, Denmark; Clone Mac 387, code no. M 0747), which shows the cytoplasm of myelomonocytic cells, certain reactive tissue macrophages, squamous mucosal, and reactive epidermis at dilution 1:50; lysozyme (DakoCytomation, Glostrup, Denmark; anti-human polyclonal rabbit; EC 3.2.1.17 Code no. A 0099) at dilution 1:700; Von Willebarnd Factor (DakoCytomation, polyclonal rabbit, anti-human; code no. A0082) to highlight endothelial cells at dilution 1:700; vimentin (DakoCytomation, Clone V9, Code-No. M 0725), which stains cells of mesodermal origin, at dilution 1:50; and smooth muscle actin (Dako, monoclonal mouse antibody, clone 1A4 Code M0851), at dilution 1:50.

FIGURE 1. Ventral view of the bull suffering from besnoitiosis. Note skin and scrotal lesions.

Besnoitia besnoiti RT-PCR

Stored biopsy material of the left femoral lymph node, sampled during necropsy and stored at –20 C, was shipped on ice via overnight air courier to the Federal Research Institute for Animal Health, Friedrich Loeffler Institut, Wusterhausen, Germany. DNA was extracted from the tissue using a commercial kit (Tissue Kit; Macherey and Nagel, Düren, Germany) as recommended by the manufacturer along with a negative processing control. RT-PCR was performed using the BbRT2 protocol with primers Bb3 and Bb6 and probe Bb3–6 (5′-FAM, 3′-BHQ1) as described (Schares et al., 2011).

RESULTS

Lesions, histopathology, tissue electron microscopy, and immunohistochemistry

Gross external lesions included thin body condition, unilateral epistaxis, conjunctival edema, diffuse subcutaneous edema of ventral head and neck, and areas of dry, cracked, hard skin, in places sloughing to expose underlying irregular erosions or ulcers affected the ventral sternum and trunk, the limbs from the elbow and stifle joints distally, and the entire scrotum (Fig. 1). Leucocytosis with left shift neutrophilia was evident in a peripheral blood smear. Main necropsy lesions included marked peripheral lymphadenomegaly due to edema and lymphoid hyperplasia, mild serous ascites, prominent submandibular,

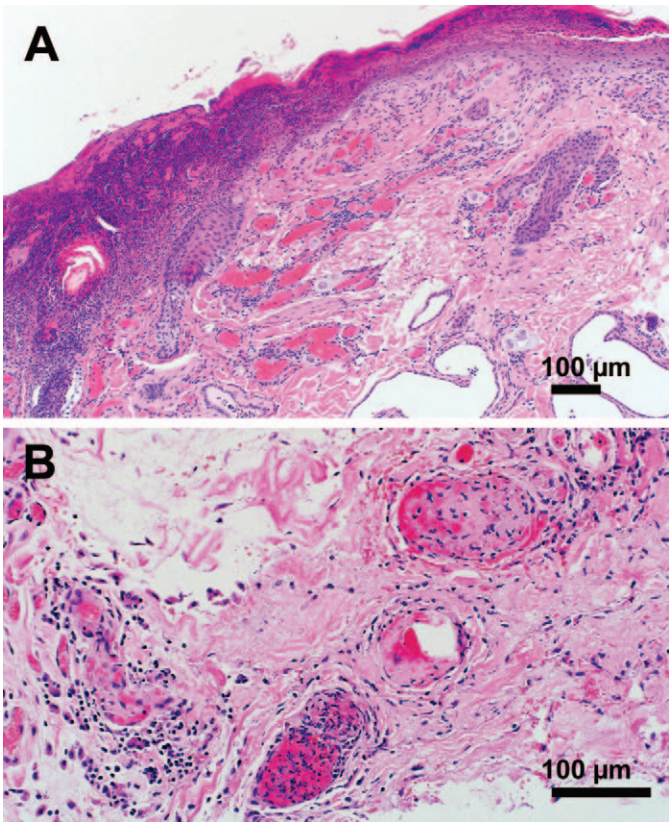

FIGURE 2. Histological sections of skin. (**A**) Scrotal skin transition from more normal to area of epidermal and dermal necrosis. (**B**) Deep subcutaneous vessels containing thromboses. H&E.

perioesophageal, peritracheal, subscapular, and some intermuscular edema, especially of the neck, and mild anasarca of affected skin, marked testicular congestion with petechiation of the epididymal tunica albuginea, diffuse renal cortical pallor and mild swelling, bladder filled with pale watery urine showing mild aciduria, glucosuria (50 mg/dl), and marked proteinuria (100–500 mg/L, Combur 9 Test, Roche Diagnostics, Ferndale 2125, Randburg, South Africa), serofibrinous hydropericardium, diffuse serous atrophy, edema and congestion of the coronary fat, abomasal mucosal edema, pulmonary edema and foam-filled trachea, pulmonary cranial lobe septal and mediastinal emphysema, bile-distended gallbladder, and marked congestion and swelling of the caudal nasopharyngeal mucosa and submucosa.

Histologically, dermal lesions were multifocal-to-coalescing, ranging from normal skin to skin showing acanthosis, orthokeratotic hyperkeratosis, superficial intracorneal pustules or full-thickness epidermal or epidermal plus dermal necrosis, with or without sloughing, and variable inflammatory reaction at the live tissue interface (Fig. 2A). These lesions were associated with no, few, or several superficial dermal protozoal tissue cysts, all at a similar stage of development, on average 1–4 peripheral round, oval, or indented vesicular nuclei, and some cysts that visibly contained parasites. Many of the tissue cysts occurred singly or in clusters, sometimes tightly adjacent to each other, in close proximity to or within walls of especially veins, often subendothelially and sometimes within venous valves. In some skin sections many tissue cysts were found in regions of normal skin between adnexal structures and with minimal or absent inflammatory response. Several tissue cysts were found in hypodermis and deep subcutaneous tissues, many in the epididymis and scattered within the testicles between the seminiferous tubules; however, they were most numerous in the pampiniform plexus (Figs. 3, 4). Diffuse interstitial lymphoplasmacytic orchitis occurred with an absence of spermatogenesis. Tissues with scattered, occasional, single parasitic cysts included lymph nodes, spleen, lung, myocardium, skeletal muscle, nasopharyngeal mucosa, and sublingual muscle, with none being found in sections of kidneys, intestinal wall, meninges, or brain.

Occasional small-to-medium diameter vessels, especially veins in the subcutis and epididymis, contained fibrin-leukocyte thrombi, sometimes organizing, and had variable mural necrosis (Fig. 2B). Leucocytes within the thrombi were often degenerated or necrotic neutrophils.

The myocardial fat was diffusely atrophied, edematous, congested, and with scattered macrophages often in clusters of smaller mononucleated cells or joining to form circles with central amorphous fatty material, presumably in the process of phagocytosing lipocytes, or as normal multinucleated giant macrophages with central nuclei and not typical of parasitic cyst cells. These cells did not contain light-microscopically, ultrastructurally, or immunohistochemically visible parasites, and they were immunohistochemically positive with MAC387, lysozyme, and vimentin antibodies. Similar macrophages were also found scattered in loose connective tissue or fat of the mesentery and the nasopharyngeal submucosa.

Renal histopathology included marked proteinuria seen as intratubular proteinaceous casts, intracytoplasmic hyaline droplets in scattered convoluted tubular cells, mild interstitial lymphoplasmacytic nephritis with some necrotic inflammatory cells, segmental multifocal vascular wall necrosis of some larger blood vessels, occasional cortico-medullary vascular mural organizing thrombi, and diffuse thickening of glomerular basement membranes with marked glomerular protein leakage into Bowman's spaces.

IMH examination revealed *Besnoitia* tissue cyst cells to be negatively staining with both macrophage antibodies and with Von Willebrand factor antibody. Vimentin stained the cytoplasm of *Besnoitia* cyst cells positively whereas smooth muscle actin staining varied from faint granular cytoplasmic staining to crisp cytoplasmic granular staining of occasional cysts. Immunoperoxidase reaction showed peripheral cytoplasmic smooth muscle actin staining of a subendothelial tissue cyst (Fig. 3). The BVD virus antibody did not elucidate virus in any of the tissues tested. The IMH did not reveal any organisms in deep subcutis blood vessels which had vasculitis and thrombosis. Parasites of any stage were not found by light microscope, various stains, or by IMH in kidneys, myocardium, and coronary fat.

Host cells ultrastructurally contained scanty peripheral cytoplasmic filaments with focal densities (Fig. 3) and abundant rough endoplasmic reticulum that displayed dilation in some instances.

TEM of renal vessels at foci of vasculitis revealed necrosis and fibrin. No parasites were found on TEM of kidneys or in coronary fat vascular endothelium, vascular tunica media, single macrophages, or in multinucleated giant macrophages.

Tissues tested by RT-PCR for the gammaherpes virus, which causes malignant cattharal fever in cattle and is also a cause of vasculitis, lymphadenomegaly, dyspnea, serous nasal to mucopu-

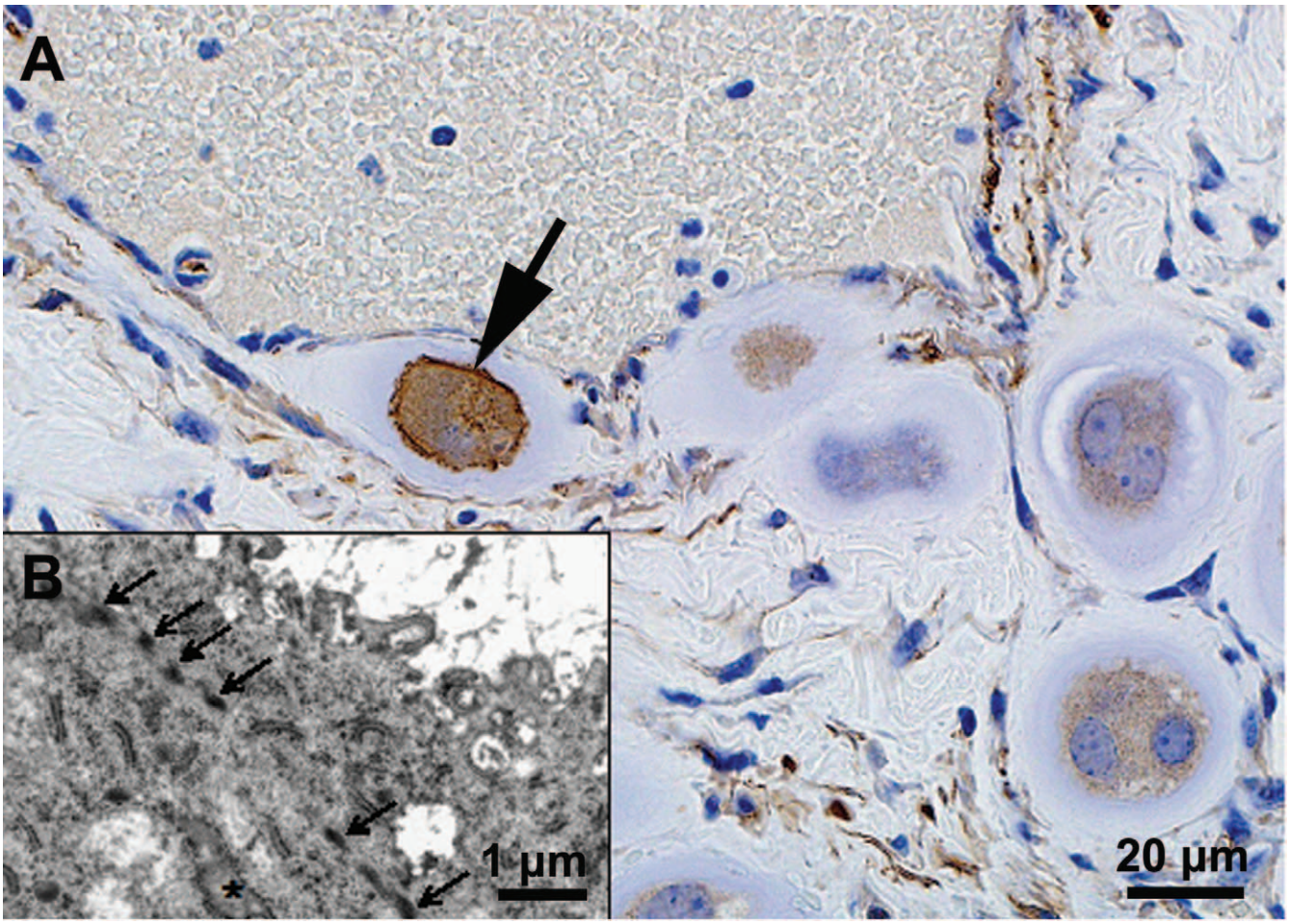

FIGURE 3. *Besnoitia* tissue cysts in scrotal subcutaneous tissue. (**A**) Immunoperoxidase staining with antibody against smooth muscle actin. Note several tissue cysts in perivascular connective tissue and a sub-endothelial cyst with peripheral cytoplasmic smooth muscle actin staining (arrow). (**B**) Inset showing TEM of host cell cytoplasm with peripheral myofilaments (arrows). Note dilated endoplasmic reticulum (asterisk).

rulent discharge, and sometimes exudative encrusted skin lesions (Reid and van Vuuren, 2004) were negative for both sheep- (OvHV-2) and wildebeest-associated (AlHV-2) virus.

DNA extracted from a femoral lymph node revealed a positive *B. besnoiti* RT-PCR (cycle of transition 31.7). The negative processing control revealed a negative RT-PCR result.

Besnoitia stages

Parasites or lesions were not seen in the first skin biopsy. In the second skin biopsy, 1 or 2 tissue cysts were seen per section. These cysts were approximately 10 μm in diameter and contained a single zoite; no lesions were associated with these cysts. The following description of *Besnoitia* stages is from tissues of the dead bull. Only a few zoites were found outside the tissue cysts after intense search of immune-stained sections (Fig. 4). Tissue cysts were 10–70 μm in diameter and contained 1–12 bradyzoites (Fig. 4). They were most numerous in affected epidermis, testicles, and the pampiniform venous plexus. Tissue cysts were commonly located in the walls of or near blood vessels, some tissue cysts were subendothelial, bulging into vascular lumens, and some appeared to be free in the blood vascular lumen. The granules in bradyzoites were stained red with PAS reaction. In sections that reacted with PAS, bradyzoites varied in size and in their intensity of PAS reaction; some were plump and others were slender (Fig. 4A–D). The PAS reactivity was more intense at the narrower end of the bradyzoites. In some bradyzoites the PAS-positive material appeared as big clumps but in others as granules. With IMH staining with *B. oryctofelisi* and BAG-1 antibodies, the staining was confined to parasites. With Gomori's silver stain only bradyzoites were stained very faintly whereas the rest of the cyst was unstained.

By TEM, tissue cysts had an outer homogenous layer, a middle layer with host cell nuclei and cytoplasm, and a third component consisting of a vacuole with parasites (Fig. 5). In the youngest tissue cysts containing 1–4 bradyzoites, bradyzoites were enclosed in an ill-defined vacuolar membrane surrounded by an electron-dense zone of host cell cytoplasm with a massive network of rough endoplasmic reticulum and a halo containing connective tissue elements, the entire structure being referred to as a tissue cyst. The organisms enclosed in the vacuolar membrane were plump to elongated and contained a varied number of different-sized amylopectin granules. The bradyzoites contained a conoid, microtubules, subpellicular microtubules, elongated mitochon-

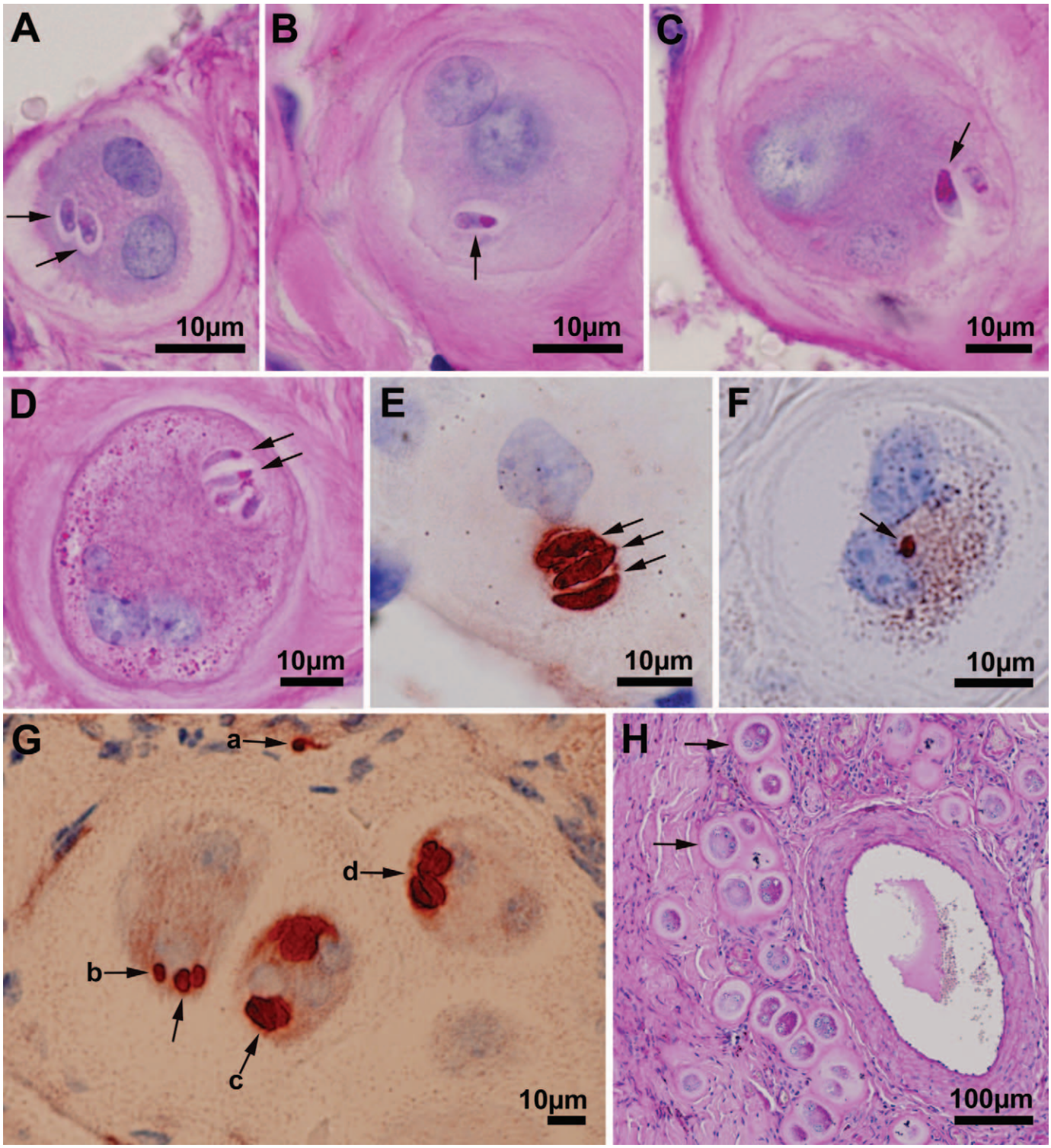

FIGURE 4. Development of *Besnoitia besnoiti* tissue cysts in histological sections of tissues of a naturally infected bull from South Africa. (**A–D**) and (**H**) stained with periodic acid Schiff (PAS) reaction counter-stained with hematoxylin, (**E**) IMH staining with *Besnoitia oryctofelisi* polyclonal rabbit antibody, (**F,G**) IMH staining with bradyzoite-specific BAG-1 antibody. (A) Two PAS-negative zoites in separate vacuoles (arrows). Note 2 host cell nuclei (hcn) and the homogenous outer layer (bar code). (B) One bradyzoite in a vacuole (arrow). Note intense PAS reaction at the narrow end of the zoite. (C) Two different-sized bradyzoites (arrows) with varying PAS reactivity. (D) Four bradyzoites in a vacuole, 2 of which are cut longitudinally (arrows). (E) Three zoites (arrows) intensely stained with *B. oryctofelisi* antibody. Note absence of staining of the vacuole and host cell elements. The zoites swell up after staining with *Besnoitia* antibody. (F) One bradyzoite (arrow) in a large tissue cyst. (G) One extracellular (a) and 3 groups of intracystic bradyzoites (b–d). Note 3 bradyzoites (arrows) in (b), apparently in different vacuoles. Groups of bradyzoites in (c) and (d) are located in separate vacuoles. (H) Numerous tissue cysts around a blood vessel in pampiniform plexus.

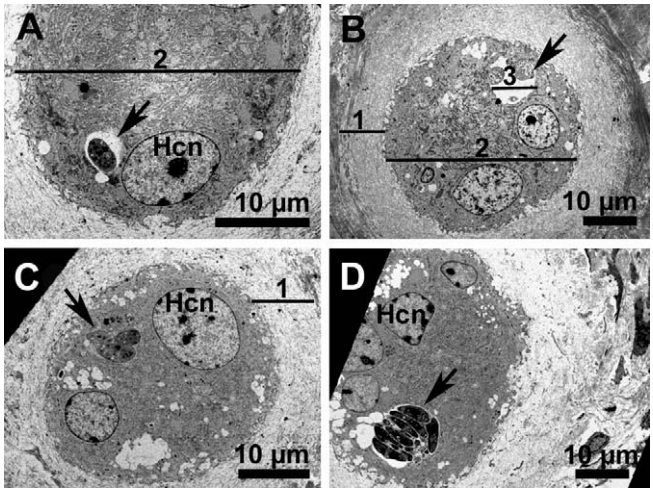

FIGURE 5. TEM of early tissue cysts of *B. besnoiti*. Note 1–7 bradyzoites enclosed in a thin parasitophorous vacuolar membrane (arrows). The outer layer (layer 1) consists of connective tissue. The middle layer (layer 2) is electron dense and contains multiple host cell nuclei (hcn). Layer 3 encloses bradyzoites. (**A**) Tissue cyst with 1 bradyzoite. (**B**) Tissue cyst with 2 bradyzoites that appear to be degenerated. (**C**) Tissue cyst with 3 bradyzoites. (**D**) Tissue cyst with 7 bradyzoites.

dria, dense granules, rhoptries, and micronemes (Figs. 6, 7). The pellicle on both sides at the conoidal end contained electron-dense material (Fig. 7). Only a few micronemes were seen in all bradyzoites examined. The contents of rhoptries were electron dense with a long neck and a bulbous portion which was turned towards the conoid in some sections (Fig. 7). The nucleus was subterminal to terminal (Fig. 6). Five longitudinally cut bradyzoites in TEM sections were 7.6–8.2 × 1.7–2.0 µm in size.

Bradyzoites from a chronic case of cutaneous besnoitiosis in South Africa revealed numerous micronemes in bradyzoites.

DISCUSSION

Tachyzoites and tissue cysts are the 2 tissue stages of *Besnoitia* species found in intermediate hosts. Tachyzoites of *Besnoitia* species are like other coccidian proliferative stages and multiply in several tissues. Tissue cysts of *Besnoitia* species are structurally intriguing because the host cell nuclei are incorporated inside the cyst and the host nuclei are hypertrophied. The *Besnoitia* tissue cyst can be divided into 3 layers or compartments; the outer layer with connective-like tissue, the middle layer incorporating host nuclei, and the cyst proper containing the bradyzoites. Using the immune-staining with *Besnoitia* polyclonal antibodies, Dubey and Lindsay (2003) showed that in *B. oryctofelisi* tissue cysts only the parasites were stained with antibodies whereas the rest of the cyst was not, suggesting the host origin of middle and outer layer. Similar results were confirmed with *B. besnoiti* cysts in the present study. The development of tissue cysts of *Besnoitia* species tissue cysts has been described from experimentally infected animals (Sheffield, 1968; Basson et al., 1970; Sénaud et al., 1974; Dubey and Lindsay, 2003; Dubey, Sreekumar et al., 2003; Dubey and Yabsley, 2010). The present study describes the development of *Besnoitia* tissue cysts for the first time in a naturally infected animal in which besnoitiosis had been confirmed by histology and by PCR.

Coccidian bradyzoites are PAS-positive because they contain numerous amylopectin granules that are rare or absent in the tachyzoite stage. Little is known of stage conversion of tachyzoite to bradyzoite in *Besnoitia*. The availability of the BAG-1 antibodies that are specific for the bradyzoite stage makes it easier to follow conversion from tachyzoites to bradyzoites; these antibodies developed against BAG-1 protein from *T. gondii* react with bradyzoites of several coccidians including *Neospora* and *Sarcocystis* but do not react with tachyzoites of any species (Dubey and Sreekumar, 2003). The polyclonal antibodies developed against tachyzoites of *B. oryctofelisi* react with other species of *Besnoitia*, including *B. besnoiti* as shown here. Dubey and Lindsay (2003) reported that zoites in young *B. oryctofelisi* tissue cysts at 12 days PI were PAS-negative and lacked amylopectin and enigmatic bodies, which is characteristic of bradyzoites in older tissue cysts. In this respect the tissue cyst formation in *B. neotomofelis* resembled that described for *B. oryctofelisi* (Dubey and Lindsay, 2003).

Until recently, little was known of the structural differences among different *Besnoitia* species (Dubey, Sreekumar et al., 2003). Recently it was reported that bradyzoites of *B. besnoiti*, *B. bennetti*, and *B. tarandi* lacked the enigmatic bodies that were considered a generic character for *Besnoitia* species (Dubey et al., 2002; Dubey, Shkap et al., 2003; Dubey, Sreekumar et al., 2003; Dubey et al., 2005). Dubey, Shkap et al. (2003) described in detail the ultrastructure of *B. besnoiti* macroscopic cysts which contained bradyzoites from a naturally infected bull from Israel. The bradyzoites contained numerous micronemes located throughout the bradyzoites. Bradyzoites from these macroscopic cysts from the bull from Israel were 6.0–7.7.5 × 1.9–2.3 µm, not much different than those in the present case from South Africa. Although not enumerated, micronemes were numerous in bradyzoites from macroscopic *B. besnoiti* tissue cysts from infected cattle from Germany (Mehlhorn et al., 2009; Majzoub et al., 2010), Israel (Shkap et al., 1988, 1995), Portugal (Cortes et al., 2006), and South Africa (as illustrated by Bigalke and Prozesky, 2004). In the present study, numerous micronemes were found in bradyzoites from tissue cysts from a chronically infected bovine from South Africa that were examined retrospectively for comparison. A review of the literature has not revealed any geographic differences in structure of mature *B. besnoiti* bradyzoites. In this respect micronemes were very few in bradyzoites of young tissue cysts examined in the present study. The same applies to the presence of amylopectin. Results of the present study indicate that micronemes and amylopectin accumulate in bradyzoites with time, and there is no reason to doubt the diagnosis of *B. besnoiti* infection in the present case.

The pathogenesis of *B. besnoiti* is not fully understood. The acute febrile stage is thought to be due to multiplication of tachyzoites in vascular endothelium and associated vasculitis. During the febrile stage, free organisms, considered to be tachyzoites, can be found in peripheral circulation (Bigalke and Prozesky, 2004); none were detected in blood smears from the acutely infected bull in the present study. Pulmonary edema and congestion (Diesing et al., 1988) and anasarca have been ascribed to the vascular damage (vasculitis and sometimes thrombosis) occurring at this stage in experimental animals (Bigalke and

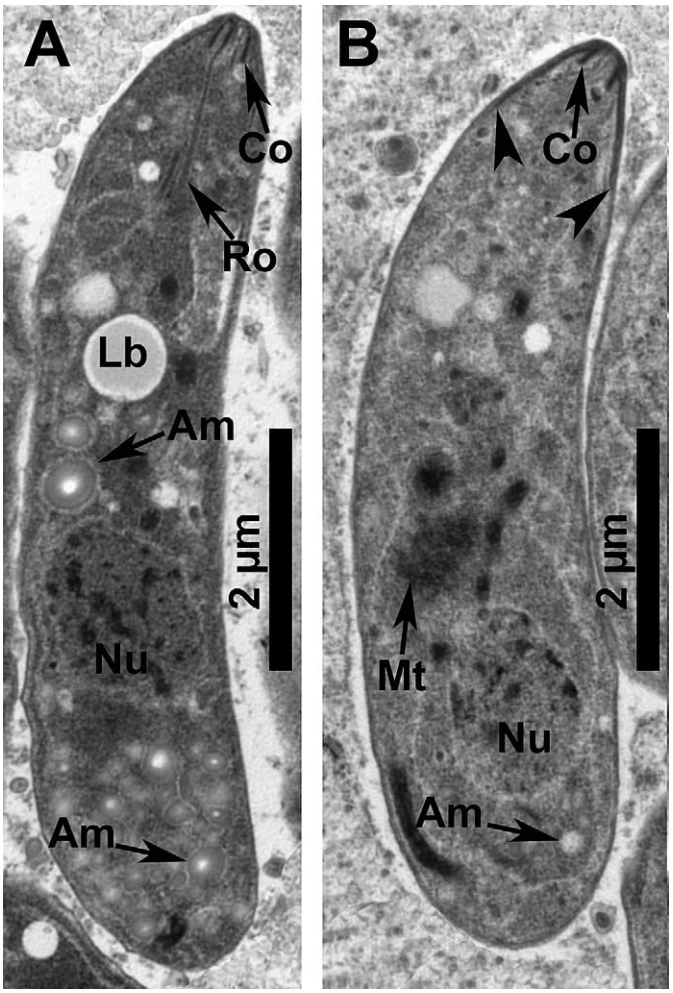

FIGURE 6. TEM of *B. besnoiti* bradyzoites. Two longitudinally cut bradyzoites (**A**, **B**) with varying position and contents of amylopectin (Am), nucleus (nu), lipid body (Lb), and mitochondria (Mt). Note conoid (Co) with thickening of the pellicle at the conoidal end (arrow heads) and rhoptries (Ro).

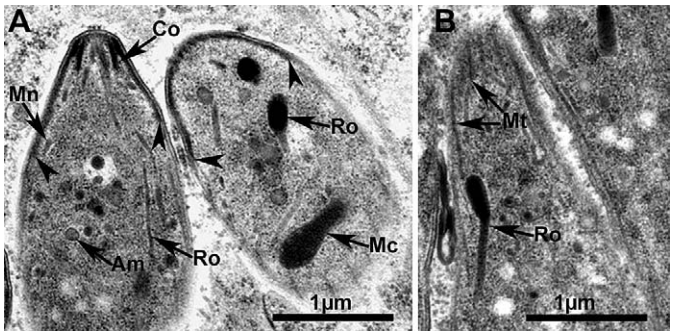

FIGURE 7. TEM of *B. besnoiti* bradyzoites. Higher magnification of conoidal ends of 3 bradyzoites. (**A**) Note conoid (Co), rhoptries (Ro) with the bulbous blind end towards the conoid, rare amylopectin (Am), few micronemes (Mn), and part of mitochondria (Mc). The pellicle is thickened towards the conoid (opposing arrowheads). (**B**) Conoidal end of a bradyzoite with subpellicular microtubules (Mt) and a rhoptry (Ro) with its blind end towards the conoid.

Prozesky, 2004), or to a possible toxic effect of the parasite causing increased vascular permeability (Bigalke and Prozesky, 2004), with no prior reports of severe hypoalbuminaemia due to nephrotic syndrome found. Only a few clinical reports in veterinary literature describe protein-losing nephrotic syndrome in cattle as a result of glomerulopathy or glomerulonephritis, and this is usually associated with renal amyloidosis (Murray and Sharp, 2009). Protein-losing glomerulopathy as a cause of anasarca in acute besnoitiosis has not been reported previously to the knowledge of the authors, and this warrants further investigation in future and archived cases.

During the chronic stage of bovine besnoitiosis only tissue cysts (no tachyzoites) are found. It is not certain if new tissue cysts are formed during the chronic stage and how long the cysts persist in cattle (Bigalke and Prozesky, 2004). Although some tissue cysts do degenerate and cause inflammation, there is no evidence that besnoitiosis can be reactivated from the chronic to acute stage (Bigalke and Prozesky, 2004). This is unlike the biology of rodent *Besnoitia* species where, for example, chronic *Besnoitia jellisoni* infection in rodents can be reactivated by experimentally-induced immunosuppression (Frenkel and Wilson, 1972; Chinchilla and Frenkel, 1978).

In the present study, the bull was RT-PCR negative for alcelaphine and ovine gammaherpes viruses causing malignant catarrhal fever in cattle, a possible differential to besnoitiosis as a cause of vasculitis, lymphadenomegaly, dyspnea, serous nasal to mucopurulent discharge, and sometimes exudative encrusted skin lesions (Reid and van Vuuren, 2004). Tissues stained immunohistochemically for BVD virus were negative as well, ruling out BVD co-infection as a differential cause of glomerulonephritis, skin lesions, vasculitis, and immunosuppression (Potgieter, 2004) .

As stated earlier, *Besnoitia* tissue cysts are structurally unusual because cells of the host are enclosed inside the "cyst." The type of host cell parasitized is assumed to be a connective tissue cell. Ayroud et al. (1995), reporting on besnoitiosis in reindeers, speculated that the cyst host cells were most likely to be fibroblasts due to the presence of the external collagenous capsule and the location of cysts in fibrous connective tissue. Bigalke and Prozesky (2004) stated that histiocytic cells in association with blood vessel walls become parasitized to form typical cysts. In the current case the typical parasitic host cells stained negatively by IMH with 2 macrophage markers and negative for Von Willebrand factor, which likely rules out endothelial cell origin, but were confirmed by positive cytoplasmic vimentin staining to be of mesodermal, most likely fibroblastic, origin. Smooth muscle actin staining of cyst cytoplasm varied from faint and finely granular to peripherally and occasionally centrally, and crisply granular in some cysts, corresponding with the distribution of focal densities and abundant rough endoplasmic reticulum found ultrastructurally that are characteristic of myofibroblasts (Ghadially, 1988). During tissue repair, fibroblasts differentiate into myofibroblasts that synthesize extracellular matrix components (Hinz, 2007; Hinz et al., 2007).

ACKNOWLEDGMENTS

Dr. Sarah Clift, Rephima Phaswane, and Naomi Timmerman are thanked for the non-*Besnoitia*-specific IMH tissue section staining. Dr. Marco Romito of the Onderstepoort Veterinary Institute is thanked for performing the PCR for the gammaherpes viruses. The Department of

Paraclinical Sciences is gratefully acknowledged for financial support. We thank Dr. Shiv Kumar Verma for graphic help.

LITERATURE CITED

Ayroud, M., F. A. Leighton, and S. V. Tessaro. 1995. The morphology and pathology of *Besnoitia* sp. in reindeer (*Rangifer tarandus tarandus*). Journal of Wildlife Diseases **31:** 319–326.

Basson, P. A., R. M. McCully, and R. D. Bigalke. 1970. Observations on the pathogenesis of bovine and antelope strains of *Besnoitia besnoiti* (Marotel, 1912) infection in cattle and rabbits. Onderstepoort Journal of Veterinary Research **37:** 105–126.

Besnoit, C., and V. Robin. 1912. Sarcosporidiose cutanée chez une vache. Revue Vétérinaire **37:** 649–663.

Bigalke, R. D. 1968. New concepts on the epidemiological features of bovine besnoitiosis as determined by laboratory and field investigations. Onderstepoort Journal of Veterinary Research **35:** 3–138.

———, and L. Prozesky. 2004. Besnotiosis. *In* Infectious diseases of livestock, 2nd ed., vol. 1, J. A. W. Coetzer, and R. C. Tustin (eds.). Oxford University Press Southern Africa, Cape Town, South Africa, p. 351–359.

Chinchilla, M., and J. K. Frenkel. 1978. Mediation of immunity to intracellular infection (*Toxoplasma* and *Besnoitia*) within somatic cells. Infection and Immunity **19:** 999–1012.

Cortes, H. C. E., Y. Reis, H. Waap, R. Vidal, H. Soares, I. Marques, I. Pereira da Fonseca, I. Fazendeiro, M. L. Ferreira, V. Caeiro et al. 2006. Isolation of *Besnoitia besnoiti* from infected cattle in Portugal. Veterinary Parasitology **141:** 226–233.

Diesing, L., A. O. Heydorn, F. R. Matuschka, C. Bauer, E. Pipano, D. T. De Waal, and F. T. Potgieter. 1988. *Besnoitia besnoiti*: Studies on the definitive host and experimental infections in cattle. Parasitology Research **75:** 114–117.

Dubey, J. P., and D. S. Lindsay. 2003. Development and ultrastructure of *Besnoitia oryctofelisi* tachyzoites, tissue cysts, bradyzoites, schizonts and merozoites. International Journal for Parasitology **33:** 807–819.

———, D. S. Lindsay, B. M. Rosenthal, C. Sreekumar, D. E. Hill, S. K. Shen, O. C. H. Kwok, L. G. Rickard, S. S. Black, and A. Rashmir-Raven. 2002. Establishment of *Besnoitia darlingi* from opossums (*Didelphis virginiana*) in experimental intermediate and definitive hosts, propagation in cell culture, and description of ultrastructural and genetic characteristics. International Journal for Parasitology **32:** 1053–1064.

———, V. Shkap, E. Pipano, L. Fish, and D. L. Fritz. 2003. Ultrastructure of *Besnoitia besnoiti* tissue cysts and bradyzoites. Journal of Eukaryotic Microbiology **50:** 240–244.

———, and C. Sreekumar. 2003. Redescription of *Hammondia hammondi* and its differentiation from *Toxoplasma gondii*. International Journal for Parasitology **33:** 1437–1453.

———, C. Sreekumar, T. Donovan, M. Rozmanec, B. M. Rosenthal, M. C. B. Vianna, W. P. Davis, and J. S. Belden. 2005. Redescription of *Besnoitia bennetti* (Protozoa: Apicomplexa) from the donkey (*Equus asinus*). International Journal for Parasitology **35:** 659–672.

———, ———, D. S. Lindsay, D. Hill, B. M. Rosenthal, L. Venturini, M. C. Venturini, and E. C. Greiner. 2003. *Besnoitia oryctofelisi* n. sp. (Protozoa: Apicomplexa) from domestic rabbits. Parasitology **126:** 521–539.

———, and M. J. Yabsley. 2010. *Besnoitia neotomofelis* n. sp. (Protozoa: Apicomplexa) from the southern plains woodrat (*Neotoma micropus*). Parasitology **137:** 1731–1747.

European Food Safety Authority. 2010. Bovine besnoitiosis: An emerging disease in Europe. EFSA Journal **8:** e1499.

Fernández-García, A., V. Risco-Castillo, S. Pedraza-Díaz, A. Aguado-Martínez, G. Álvarez-García, and M. Gómez-Bautista. 2009. First isolation of *Besnoitia besnoiti* from a chronically infected cow in Spain. Journal of Parasitology **95:** 474–476.

Frenkel, J. K., and H. R. Wilson. 1972. Effects of radiation on specific cellular immunities: besnoitiosis and a herpesvirus infection of hamsters. Journal of Infectious Diseases **125:** 216–230.

Gentile, A., G. Militerno, G. Schares, A. Nanni, S. Testoni, P. Bassi, and N. S. Gollnick. 2012. Evidence for bovine besnoitiosis being endemic in Italy—First *in vitro* isolation of *Besnoitia besnoiti* from cattle born in Italy. Veterinary Parasitology **194:** 108–115.

Ghadially, F. N. 1988. Ultrastructural pathology of the cell and matrix, vol. 2, 3rd ed. Butterworths, London, U.K., 1340 p.

Haines, D. M, and B. J. Chelack. 1991. Technical considerations for developing enzyme immunohistochemical staining procedures on formalin-fixed paraffin-embedded tissues for diagnostic pathology. Journal of Veterinary Diagnostic Investigation **3:** 101–112.

Hayat, M. A. 2000. Principles and techniques of electron microscopy. Biological applications, 4th ed. Cambridge University Press, Cambridge, U.K., 564 p.

Hinz, B. 2007. Formation and function of the myofibroblast during tissue repair. Journal of Investigative Dermatology **127:** 526–537.

———, S. H. Phan, V. J. Thannickal, A. Galli, M. L. Bochaton-Piallat, and G. Gabbiani. 2007. The myofibroblast: One function, multiple origins. American Journal of Pathology **170:** 1807–1816.

Jacquiet, P., E. Liénard, and M. Franc. 2010. Bovine besnoitiosis: Epidemiological and clinical aspects. Veterinary Parasitology **174:** 30–36.

Majzoub, M., W. Breuer, N. S. Gollnick, A. Rostaher, G. Schares, and W. Hermanns. 2010. Ein Ausbruch von Besnoitiose bei Rindern in Deutschland: Pathomorphologische, ultrastrukturelle und molekularbiologische Untersuchungen. Wiener Tierärztliche Monatsschrift **97:** 9–15.

McAllister, M. M., S. F. Parmley, L. M. Weiss, V. J. Welch, and A. M. McGuire. 1996. An immunohistochemical method for detecting bradyzoite antigen (BAG5) in *Toxoplasma gondii*-infected tissues cross-reacts with a *Neospora caninum* bradyzoite antigen. Journal of Parasitology **82:** 354–355.

Mehlhorn, H., S. Klimpel, and E. Schein. 2009. Another African disease in Central Europa: Besnoitiosis of cattle. I. Light and electron microscopical study. Parasitology Research **104:** 861–868.

Murray, G. M., and A. E. Sharp. 2009. Nephrotic syndrome due to glomerulopathy in an Irish dairy cow. Veterinary Record **164:** 179–180.

Pols, J. W. 1960. Studies on bovine besnoitiosis with special reference to the aetiology. Onderstepoort Journal of Veterinary Research **28:** 265–356.

Potgieter, L. D. N. 2004. Bovine viral diarrhoea and mucosal disease. *In* Infectious diseases of livestock, 2nd ed., vol. 2, J. A. W. Coetzer, and R. C. Tustin (eds.). Oxford University Press Southern Africa, Cape Town, South Africa, p. 946–969.

Reid, H. W., and M. van Vuuren. 2004. Malignant catarrhal fever. *In* Infectious diseases of livestock, 2nd ed., Vol. 2, J. A. W. Coetzer, and R. C Tustin (eds.). Oxford University Press Southern Africa, Cape Town, South Africa, p. 895–907.

Rostaher, A., R. S. Mueller, M. Majzoub, G. Schares, and N. S. Gollnick. 2010. Bovine besnoitiosis in Germany. Veterinary Dermatology **21:** 329–334.

Schares, G., W. Basso, M. Majzoub, H. C. E. Cortes, A. Rostaher, J. Selmair, W. Hermanns, F. J. Conraths, and N. S. Gollnick. 2009. First *in vitro* isolation of *Besnoitia besnoiti* from chronically infected cattle in Germany. Veterinary Parasitology **163:** 315–322.

———, A. Maksimov, W. Basso, G. More, J. P. Dubey, B. Rosenthal, M. Majzoub, A. Rostaher, J. Selmair, M. C. Langenmayer et al. 2011. Quantitative real time polymerase chain reaction assays for the sensitive detection of *Besnoitia besnoiti* infection in cattle. Veterinary Parasitology **178:** 208–216.

Sénaud, J., H. Mehlhorn, and E. Scholtyseck. 1974. *Besnoitia jellisoni* in macrophages and cysts from experimentally infected laboratory mice. Journal of Protozoology **21:** 715–720.

Sheffield, H. G. 1968. Observations on the fine structure of the "cyst stage" of *Besnoitia jellisoni*. Journal of Protozoology **15:** 685–693.

Shkap, V., F. R. Matuschka, B. Yakobson, S. Perl, M. Frank, and E. Pipano. 1995. Differentiating between *Besnoitia besnoiti* from cattle and *Sarcocystis hoarensis* from rodents. Parasitology Research **81:** 490–493.

———, B. A. Yakobson, and E. Pipano. 1988. Transmission and scanning electron microscopy of *Besnoitia besnoiti*. International Journal for Parasitology **18:** 761–766.